Received: 22 March 2024 | Accepted: 12 August 2024

DOI: 10.1002/prp2.70003

SHORT REPORT

IS4-FAM, a fluorescent tool to study CXCR4 affinity and competitive antagonism in native cancer cells

Isabel Hamshaw | Marco M. D. Cominetti | Princess Nana-Akyin | Ernie Ho Yee Ho | Mark Searcey | Anja Mueller

School of Pharmacy, University of East Anglia, Norwich, UK

Correspondence
Anja Mueller, School of Pharmacy, University of East Anglia, Norwich, UK.
Email: anja.mueller@uea.ac.uk

Funding information
UKRI Biotechnology and Biological Sciences Research Council Norwich Research Park Biosciences Doctoral Training Partnership, Grant/Award Number: BB/T008717/1

Abstract

The ability to accurately measure drug-target interaction is critical for the discovery of new therapeutics. Classical pharmacological bioassays such as radioligand or fluorescent ligand binding assays can define the affinity or K_d of a ligand for a receptor with the lower the K_d, the stronger the binding and the higher the affinity. However, in many drug discovery laboratories today, the target of interest if often artificially upregulated by means of transfection to modify the host cell's genetic makeup. This then potentially invalidates the assumptions of classical pharmacology affinity calculations as the receptor of interest is no longer at normal physiological densities. The CXCR4 receptor is expressed on many different cancer cell types and is associated with metastasis and poor prognosis. Therefore, the CXCR4 receptor is a desirable target for novel therapeutics. In this study, we explore the applicability of the newly developed fluorescently tagged CXCR4 antagonists, IS4-FAM as an investigative tool to study CXCR4 affinity and competitive antagonism in native, non-transfected cancer cells using confocal microscopy and flow cytometry. IS4-FAM directly labels CXCR4 in several cell lines including high CXCR4 expressing SK-MEL-28 (malignant melanoma) and PC3 (metastatic prostate cancer) and lower CXCR4 expressing THP-1 (acute monocytic leukemia) and was competitive with the established CXCR4 antagonist, AMD3100. This highlights the potential of IS4-FAM as a pharmacological tool for drug discovery in native cells lines and tissues.

KEYWORDS

antagonist, chemokine receptor, CXCL12, CXCR4

1 | INTRODUCTION

Accurately measuring the binding of a drug to a receptor is a fundamental concept of quantitative pharmacology and the discovery of novel potent therapeutics.[1] Traditionally, drug kinetics was studied by directly measuring receptor binding using radioligands. However, the emergence of fluorescence-based binding assays offers a safer and more high-throughput method of determining drug-receptor binding kinetics.[2] In either case, binding affinity can be defined by the equilibrium dissociation constant, K_d where the lower the K_d, the stronger the binding and the higher the affinity. However, there are several challenges faced in drug discovery laboratories today due to assays

Abbreviations: CuAAC, copper-catalyzed-azide-alkyne cycloaddition; FAM, fluorescein amidites; mAb, monoclonal antibody.

being performed under very restricted conditions. This includes, but is not limited to, usings membranes rather than whole cells or usings transfected cell lines to artificially express high levels of the protein of interest.[3,4] This potentially invalidates the assumptions of classical pharmacology affinity calculations as the receptor of interest is no longer at normal physiological densities.[3] This highlights just one of the problems of modern drug discovery and in part implicates why there is such a high failure rate when taking a drug from bench to bedside.

Chemokines (small 8–12 kDa peptides) and their associated receptors play a major role in cancer survival, progression, and metastasis.[5] These small signaling molecules enable cognate chemokine receptor expressing cells to migrate along a concentration gradient to sites of infection, injury, or to secondary lymphoid organs for maturation.[6,7] One chemokine receptor, CXCR4, is commonly expressed on most hematopoietic cells and plays a significant role in neutrophil homeostasis.[8,9] The CXCR4 receptor is also detected in many types of human cancers with the thought that cancer cells can "hijack" the CXCR4/CXCL12 signaling axis in order to metastasis to secondary CXCL12 expressing sites such as the bone marrow, brain, lungs, and liver.[9] This makes CXCR4 a highly desirable therapeutic target.

IS4-FAM is a potent CXCR4 antagonist that is made via copper (I) catalyzed-azide-alkyne-cycloaddition (CuAAC) reaction between a suitably substituted peptide that binds with high affinity to CXCR4 and a FAM fluorophore.[10] In our previous study,[10] we determined that the novel compound, IS4-FAM, was not cytotoxic, it inhibited CXCL12-stimulated cancer cell migration and intracellular Ca^{2+} release in various CXCR4-expressing cancer cell types and that it exhibited greater potency over other CXCR4 antagonists.

In this study, we explored the use of IS4-FAM in three native, non-transfected cancer cell lines including high CXCR4 expressing SK-MEL-28 (malignant melanoma) and PC3 (metastatic prostate cancer) and lower CXCR4 expressing THP-1 (acute monocytic leukemia). IS4-FAM directly labeled CXCR4 in all cell lines producing CXCR4-based fluorescent images that are comparable to the gold standard use of monoclonal antibodies (mAb). Furthermore, IS4-FAM was competitive with the established CXCR4 antagonist, AMD3100. Overall, this highlights the potential use of IS4-FAM as an investigative pharmacological tool for the study of CXCR4 and drug discovery in native cell lines and tissues.

2 | MATERIALS AND METHODS

2.1 | Cell culture

SK-MEL-28 (malignant melanoma) and THP-1 (acute monocytic leukemia) were cultured as previously described in[11] and PC3 (metastatic prostate cancer derived from an adenocarcinoma in the bone) as described in.[12] All cells were purchased from ATCC (Teddington, UK) then grown in 75 cm^3 flasks (ThermoFisher Scientific, Loughborough, UK) using Roswell Park Memorial Institute (RPMI) medium (Biosera, Nuaille, France) supplemented with 10% v/v fetal bovine serum (Invitrogen, Paisley, UK) 2 mM L-glutamine (Invitrogen, Paisley, UK) and 100 μM non-essential amino acids (Gibco, ThermoFisher Scientific, Loughborough, UK) and maintained at 37°C in a 95%/5% air/CO_2-humidified environment.

2.2 | Materials

AMD3100 was purchased from Santa Cruz Biotechnology (Heidelberg, Germany). The design and synthesis of IS4-FAM is discussed in detail in.[10] CXCL12 was purchased from Peprotech (London, UK).

2.3 | Confocal microscopy

Cells were seeded at a density of 1×10^5 mL^{-1} in RPMI media for 24 h at 37°C in a 5% CO_2 humidified environment. Cells were washed in PBS then incubated with mouse anti-CXCR4 4G10 (1:200, Santa Cruz Biotechnology, Heidelberg, Germany) and 1 μM IS4-FAM for 1 h at 4°C. Cells were washed then incubated with goat anti-mouse IgG Alexa Fluor® 568 antibody (1:200, Abcam, Cambridge, UK) for 1 h at 4°C. Finally, DAPI (1:1000, Sigma Aldrich, Hertfordshire, UK) was added for 10 min at 4°C before being washed and mounted with DPX mountant (ThermoFisher Scientific, Loughborough, UK). Slides were imaged using a Zeiss LSM 980-Airyscan 2 confocal laser scanning microscope with associated Zen 3.1 (Blue) software at 100x objective.

2.4 | Flow cytometry

All cells were harvested at a density of 1×10^6 mL^{-1} in 0.5% BSA/PBS (ThermoFisher Scientific, Loughborough, UK). Cells were washed in ice-cold PBS then incubated with mouse anti-CXCR4 4G10 (1:200) for 1 h at 4°C. Cells were washed in ice-cold PBS then incubated with goat anti-mouse IgG Alexa Fluor® 488 antibody (1:200) or 1 μM IS4-FAM for 1 h at 4°C. After incubation, cells were washed in ice-cold PBS then analyzed using a CytoFLEX and the associated CytExpert (v2.4) software (Beckman Coulter).

2.4.1 | Saturation

As previous except cells were incubated with half log concentration of IS4-FAM (10 nM to 1000 μM) for 1 h at room temperature in the dark. No IS4-FAM was added for the negative control.

2.4.2 | Competition

As previous except cells were incubated with half log concentration of IS4-FAM (10 nM to 1000 μM) plus 1 μM AMD3100 or 100 μM AMD3100 for 1 h at room temperature in the dark.

2.4.3 | Data analysis

Fluorescence was measured with a blue 488 nm laser using the FITC channel. Cell populations were plotted as forward scatter-area (FSC-A) versus side scatter-area (SSC-A) to gate the desired population and as FSC-A versus forward scatter-height (FSC-H) to gate singlets. 10 000 cell events were recorded as median fluorescence-area and plotted as receptor expression (sample/negative) using GraphPad Prism 8 software. CXCR4 expression was calculated as sample/negative control. Saturation-binding curves were fitted using one site—total with background constrained to 0. Statistical significance was calculated with one way ANOVA with post hoc Dunnett's multiple comparison test or two-way ANOVA with AMD3100 as the between measures variable.

2.5 | Nomenclature of targets and ligands

Key protein targets and ligands in this article are hyperlinked to corresponding entries in https://www.guidetopharmacology.org, the common portal for data from the IUPHAR/BPS Guide to PHARMACOLOGY,[13] and are permanently archived in the Concise Guide to PHARMACOLOGY 2019/20 (Alexander et al., 201).[14]

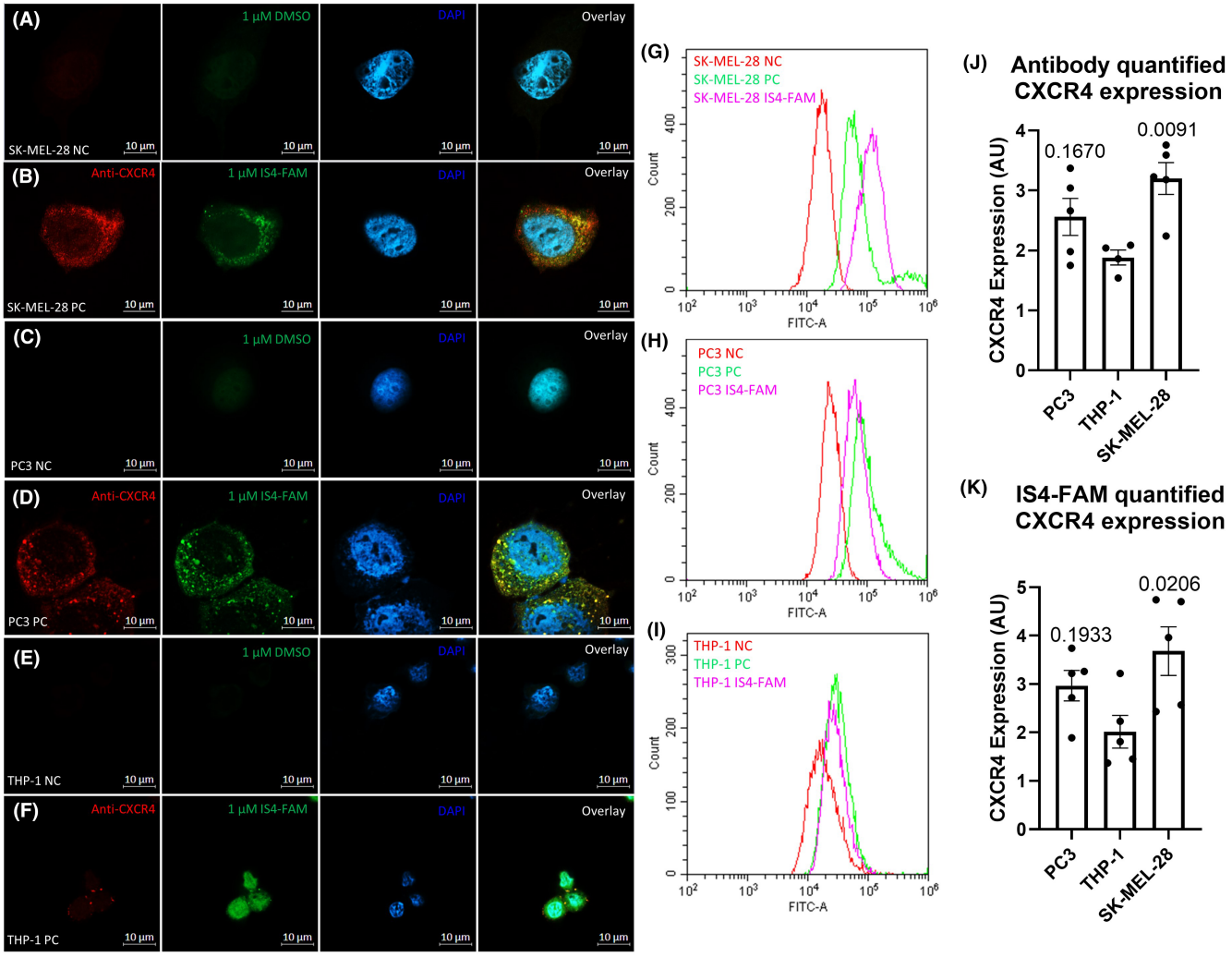

FIGURE 1 CXCR4 expression in SK-MEL-28, PC3, and THP-1 cell lines labeled using mouse anti-CXCR4 antibody (4G10) and 1 μM IS4-FAM. Confocal images of a central *Z*-stack of (A, B) SK-MEL-28, (C, D) PC3 and (E, F) THP-1 cells. Negative controls (NC; A, C, E) visualized using goat anti-mouse Alexa Fluor® 568 (red) and DAPI (blue). Positive controls (PC; B, D, F) visualized using anti-CXCR4 (4G10) with secondary goat anti-mouse Alexa Fluor® 568 (red), 1 μM IS4-FAM (green) and DAPI (blue). Data shows representative images from three independent experiments with similar findings using 100x objective. Representative histogram of CXCR4 expression in (G) SK-MEL-28 (H) PC3 and (I) THP-1 cells where negative control (red), positive control visualized using 4G10 and secondary goat anti-mouse Alexa Fluor® 488 (green) and 1 μM IS4-FAM (pink). CXCR4 expression was quantified using values acquired by (J) antibody and (K) IS4-FAM. Data are mean ± SEM, $N = 5$ and were analyzed using one-way ANOVA with post hoc Dunnett's multiple comparison test comparing conditions to THP-1. Outliers excluded using Grubbs (Alpha = 0.05).

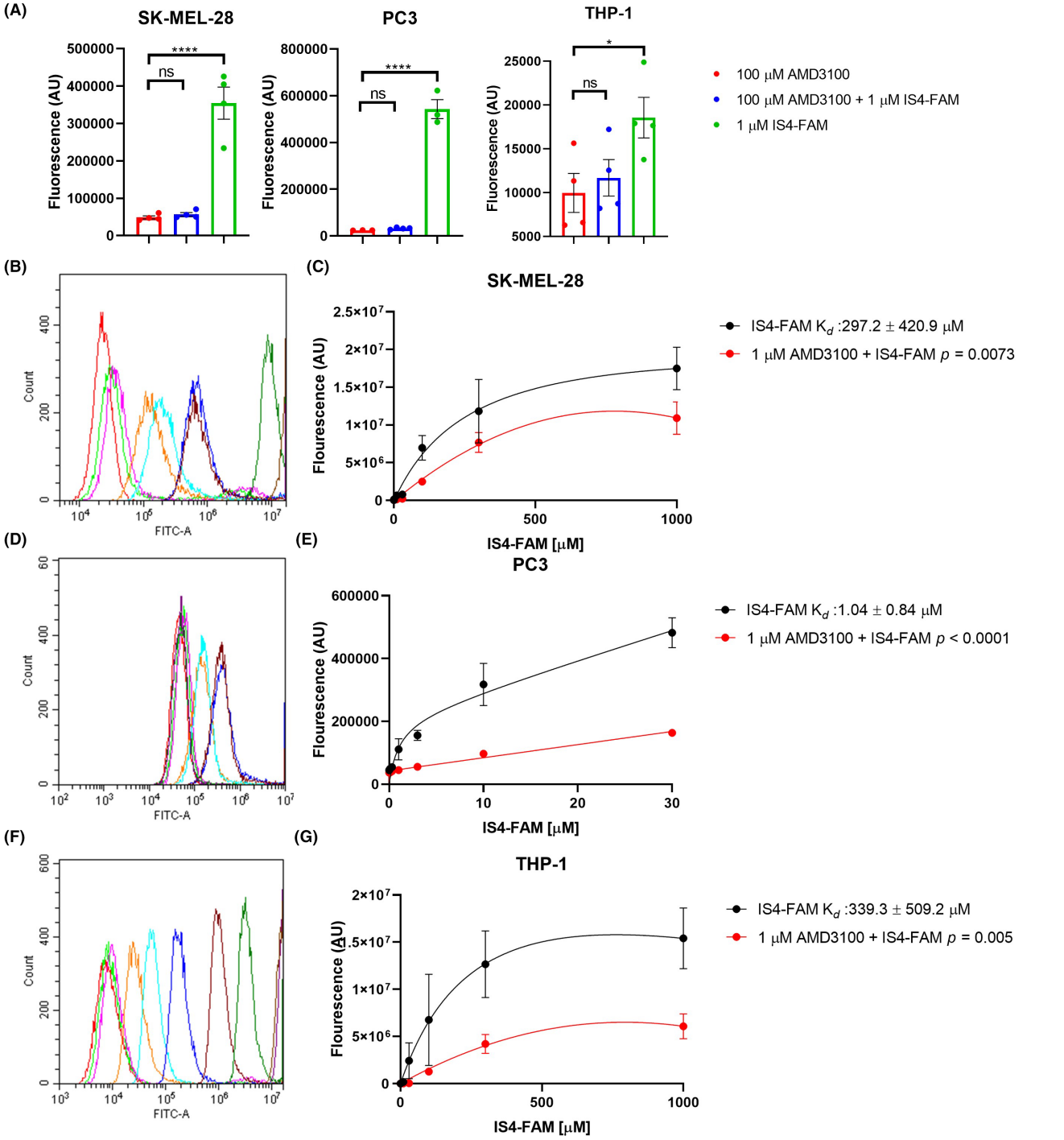

FIGURE 2 Saturation and competition binding of IS4-FAM in SK-MEL-28, PC3 and THP-1 cells. (A) Cells were treated with 100 μM AMD3100 and 1 μM IS4-FAM to determine non-specific binding. Data are mean ± SEM, $N = 4$ and were analyzed using one-way ANOVA with post hoc Dunnett's multiple comparison test comparing conditions to 100 μM AMD3100. Outliers excluded using Grubbs (Alpha = 0.05). (B) Representative histogram of SK-MEL-28 cells with no IS4-FAM (red), 100 nM IS4-FAM (green), 300 nM IS4-FAM (pink), 1 μM IS4-FAM (orange), 3 μM IS4-FAM (turquoise), 10 μM IS4-FAM (blue), 30 μM IS4-FAM (maroon), 100 μM IS4-FAM (dark green), 300 μM IS4-FAM (purple), and 1000 μM IS4-FAM (brown). (C) Saturation and competition binding curves of SK-MEL-28 cells with 10 nM to 1000 μM IS4-FAM ± 1 μM AMD3100. (D) Representative histogram of PC3 cells with no IS4-FAM (red), 10 nM IS4-FAM (dark green), 30 nM IS4-FAM (purple), 100 nM IS4-FAM (green), 300 nM IS4-FAM (pink), 1 μM IS4-FAM (orange), 3 μM IS4-FAM (turquoise), 10 μM IS4-FAM (blue), and 30 μM IS4-FAM (maroon). (E) Saturation and competition binding curves of PC3 cells with 10 nM to 30 μM IS4-FAM ± 1 μM AMD3100. (F) Representative histogram of THP-1 cells with no IS4-FAM (red), 100 nM IS4-FAM (green), 300 nM IS4-FAM (pink), 1 μM IS4-FAM (orange), 3 μM IS4-FAM (turquoise), 10 μM IS4-FAM (blue), 30 μM IS4-FAM (maroon), 100 μM IS4-FAM (dark green), 300 μM IS4-FAM (purple), and 1000 μM IS4-FAM (brown). (G) Saturation and competition binding curves of THP-1 cells with 10 nM to 1000 μM IS4-FAM ± 1 μM AMD3100. Data are mean ± SEM, $N = 4$ and were analyzed by two-way ANOVA with AMD3100 as the between measures variable.

3 | RESULTS

IS4-FAM is made via CuAAC reaction between a high CXCR4 affinity peptide and to the commercially available fluorescent dye FAM azide as the 5-isomer, that excites/emits at 490/525 nm.[10] 1 μM IS4-FAM was used to label SK-MEL-28, PC3, and THP-1 cells in comparison to mouse 4G10 anti-CXCR4 mAb plus anti-mouse Alexa Fluor® 488 binding (Figure 1). To confirm that the fluorescence seen was due to labelling on the extracellular surface of these cells, *Z*-stacks were created via confocal microscopy and central cross-sections of the cells were taken. This demonstrated that IS4-FAM was binding extracellularly with limited CXCR4 receptor internalization.

Furthermore, flow cytometry was utilized to determine the affinity of IS4-FAM in SK-MEL-28, PC3, and THP-1 cells in addition to determining if IS4-FAM was competitive with the literature CXCR4 antagonists AMD3100 (Figure 2). Non-specific binding was determined using high concentration AMD3100 in the presence of 1 μM IS4-FAM where data was found not to be significant. Half log incremental concentrations of IS4-FAM (10 nM to 1000 μM) were used to calculate a K_d of 297.2 ± 420.9 μM in SK-MEL-28 cells. Similarly, in THP-1 cells the K_d was calculated as 339.3 ± 509.2 μM and in PC3 cells, K_d was 1.04 ± 0.84 μM. The addition of 1 μM AMD3100 caused a significant decrease in fluorescence In all cell lines. These findings were validated using confocal microscopy whereby cells were incubated with 1 μM IS4-FAM in addition to 1 μM AMD3100 (Figure 3).

4 | DISCUSSION

CXCR4 is expressed in many cancers and often leads to poor survival due to the increased metastatic potential of the cancer.[9] While this makes CXCR4 a highly desirable therapeutic target, little progress has been made from bench to the bedside due to poor outcomes

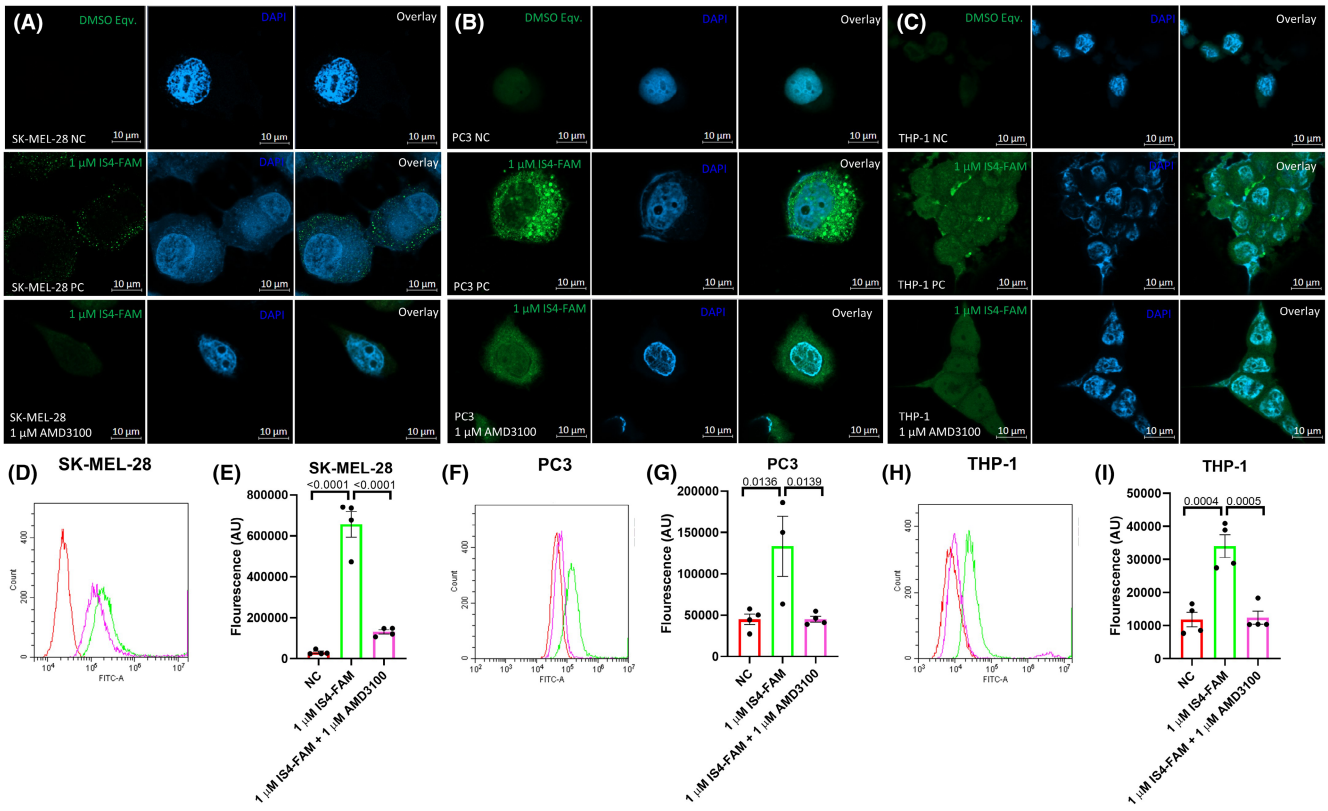

FIGURE 3 Competitive binding of 1 μM IS4-FAM with 1 μM AMD3100 in SK-MEL-28, PC3 and THP-1 cells. Confocal images of a central *Z*-stack of (A) SK-MEL-28, (B) PC3, and (C) THP-1 cells. Negative controls (NC) visualized using 1 μM DMSO and DAPI (blue). Positive controls (PC) visualized using 1 μM IS4-FAM (green) and DAPI (blue) and competitive binding using 1 μM IS4-FAM plus 1 μM AMD3100. Data shows representative images from three independent experiments with similar findings at 100x objective. (D) Representative histogram of SK-MEL-28 cells with no CXCR4 antagonists (red), 1 μM IS4-FAM (green) and 1 μM IS4-FAM + 1 μM AMD3100 (pink) with associated graphical representation shown in (E). (F) Representative histogram of PC3 cells with no CXCR4 antagonists (red), 1 μM IS4-FAM (green) and 1 μM IS4-FAM + 1 μM AMD3100 (pink) with associated graphical representation shown in (G). (H) Representative histogram of THP-1 cells with no CXCR4 antagonists (red), 1 μM IS4-FAM (green) and 1 μM IS4-FAM + 1 μM AMD3100 (pink) with associated graphical representation shown in (I). Data are mean ± SEM, $N = 4$ and were analyzed using one-way ANOVA with post hoc Dunnett's multiple comparison test comparing conditions to 1 μM IS4-FAM.

in pre-clinical trials because of low efficacy, high toxicity, or poor pharmacokinetic properties.[15] This highlights the importance of investigating novel CXCR4 based research tools to prevent further research and trial failures.

In this study we determined that IS4-FAM can directly label CXCR4 receptors expressed on SK-MEL-28, PC3, and THP-1 cells as compared to mouse 4G10 anti-CXCR4 mAb plus goat anti-mouse Alexa Fluor® 568 (Figure 1). Furthermore, the binding of IS4-FAM to CXCR4 did not induce receptor internalization indicating that IS4-FAM can be used for cell surface receptor imaging and analysis purposes.

High concentration (100 μM) of the CXCR4 antagonist AMD3100 was used to determine if IS4-FAM caused any non-specific binding. As discussed in Hamshaw et al.[10] AMD3100 and IS4-FAM bind to the same ligand binding pocket on CXCR4 therefore, pre-incubation with 100 μM AMD3100 prevents IS4-FAM from binding. Results from these experiments confirmed that IS4-FAM binds specifically to CXCR4 with no significant non-specific binding in all cell lines (Figure 2A).

The binding affinity of IS4-FAM for CXCR4, was similar for SK-MEL-28 (297.2 ± 420.9 μM) and THP-1 cells (339.3 ± 509.2 μM) while K_d was measured as 1.04 ± 0.84 μM in PC3 cells (Figure 2B–G). All cell lines were measured at the same 1-h time point using endpoint-based flow cytometry. However, as discussed in Spiegelberg et al.,[16] this technique assumes that this incubation time is sufficient to reach ligand (L), receptor binding equilibrium (K_d = [L][R]/[LR]) which can take hours to reach, especially at low concentration of ligand. For validation, future work should use the kinetic parameters k_{on} and k_{off} to determine if equilibrium has been reached through techniques such as surface plasmon resonance.

Finally, using equivalent concentrations of AMD3100 and IS4-FAM (1 μM) it was determined that IS4-FAM was competitive for the CXCR4 receptor (Figures 2B–G and 3). Therefore, IS4-FAM can successfully be used as an investigative pharmacological research tool for the study of CXCR4 in native cells lines and tissues.

AUTHOR CONTRIBUTIONS

Isabel Hamshaw: Conceptualization, data curation, formal analysis, funding acquisition, investigation, methodology, project administration, supervision, writing—original draft. **Marco M. D. Cominetti**: Conceptualization, methodology, resources, writing review & editing. **Princess Nana-Akyin** and **Ernie Ho Yee Ho**: Data curation and formal analysis. **Mark Searcey**: Conceptualization, resources and writing review & editing. **Anja Mueller**: Conceptualization, resources, software and writing review & editing.

ACKNOWLEDGMENTS

We thank Dr James McColl at the Henry Wellcome Laboratory for Cellular Imaging for the training and technical assistance provided regarding microscopy image acquisition.

FUNDING INFORMATION

This research was supported by an Undergraduate Summer Internship Scheme bursary from the UKRI Biotechnology and Biological Sciences Research Council Norwich Research Park Biosciences Doctoral Training Partnership (Grant number BB/T008717/1).

CONFLICT OF INTEREST

The authors declare that they have no conflicts of interest with the contents of this article.

DATA AVAILABILITY STATEMENT

The datasets generated during and/or analyzed during the current study are available from the corresponding author on reasonable request.

ETHICS STATEMENT

Not applicable.

ORCID

Anja Mueller https://orcid.org/0000-0003-0774-0434

REFERENCES

1. Neubig RR, Spedding M, Kenakin T, Christopoulos A. International Union of Pharmacology Committee on receptor nomenclature and drug classification. XXXVIII. Update on terms and symbols in quantitative pharmacology. *Pharmacol Rev*. 2003;55(4):597-606.
2. Sykes DA, Stoddart LA, Kilpatrick LE, Hill SJ. Binding kinetics of ligands acting at GPCRs. *Mol Cell Endocrinol*. 2019;485:9-19.
3. Hoare SR. The problems of applying classical pharmacology analysis to modern in vitro drug discovery assays: slow binding kinetics and high target concentration. *Slas Discovery*. 2021;26(7):835-850.
4. Hulme EC, Trevethick MA. Ligand binding assays at equilibrium: validation and interpretation. *Br J Pharmacol*. 2010;161(6):1219-1237.
5. Sarvaiya PJ, Guo D, Ulasov I, Gabikian P, Lesniak MS. Chemokines in tumor progression and metastasis. *Oncotarget*. 2013;4(12):2171-2185.
6. Laing KJ, Secombes CJ. Chemokines. *Dev Comp Immunol*. 2004;28(5):443-460.
7. Teicher BA, Fricker SP. CXCL12 (SDF-1)/CXCR4 pathway in cancer. *Clin Cancer Res*. 2010;16(11):2927-2931.
8. Eash KJ, Means JM, White DW, Link DC. CXCR4 is a key regulator of neutrophil release from the bone marrow under basal and stress granulopoiesis conditions. *Blood*. 2009;113(19):4711-4719.
9. Chatterjee S, Azad BB, Nimmagadda S. The intricate role of CXCR4 in cancer. *Adv Cancer Res*. 2014;124:31-82.
10. Hamshaw I, Cominetti MM, Lai W-Y, Searcey M, Mueller A. The development of potent, competitive CXCR4 antagonists for the prevention of cancer metastasis. *Biochem Pharmacol*. 2023;218:115921.
11. Hamshaw I, Ellahouny Y, Malusickis A, Newman L, Ortiz-Jacobs D, Mueller A. The role of PKC and PKD in CXCL12 and CXCL13 directed malignant melanoma and acute monocytic leukemic cancer cell migration. *Cell Signal*. 2024;113:110966.
12. Hamshaw I, Ajdarirad M, Mueller A. The role of PKC and PKD in CXCL12 directed prostate cancer migration. *Biochem Biophys Res Commun*. 2019;519(1):86-92.
13. Harding SD, Sharman JL, Faccenda E, et al. The IUPHAR/BPS guide to pharmacology in 2019: updates and expansion to encompass the new guide to immunopharmacology. *Nucleic Acids Res*. 2018;46:D1091-D1106. doi:10.1093/nar/gkx1121
14. Alexander SPH, Christopoulos A, Davenport AP, et al. The Concise Guide to PHARMACOLOGY 2023/24: G protein-coupled

receptors. *Br J Pharmacol*. 2023;180(Suppl 2):S23-S144. doi:10.1111/bph.16177

14. Caspar B, Cocchiara P, Melet A, et al. Cxcr4 as a novel target in immunology: moving away from typical antagonists. *Future Drug Discovery*. 2022;4(2):FDD77.
15. Spiegelberg D, Stenberg J, Richalet P, Vanhove M. KD determination from time-resolved experiments on live cells with LigandTracer and reconciliation with end-point flow cytometry measurements. *Eur Biophys J*. 2021;50(7):979-991.

How to cite this article: Hamshaw I, Cominetti MMD, Nana-Akyin P, Yee Ho EH, Searcey M, Mueller A. IS4-FAM, a fluorescent tool to study CXCR4 affinity and competitive antagonism in native cancer cells. *Pharmacol Res Perspect*. 2024;12:e70003. doi:10.1002/prp2.70003